

Review

# Study of sound localization by owls and its relevance to humans<sup>☆</sup>

Masakazu Konishi

*Division of Biology 216-76, California Institute of Technology, Pasadena, CA 91125, USA*

Received 31 December 1999; accepted 24 May 2000

## Abstract

Human psychoacoustical studies have been the main sources of information from which the brain mechanisms of sound localization are inferred. The value of animal models would be limited, if humans and the animals did not share the same perceptual experience and the neural mechanisms for it. Barn owls and humans use the same method of computing interaural time differences for localization in the horizontal plane. The behavioral performance of owls and its neural bases are consistent with some of the theories developed for human sound localization. Neural theories of sound localization largely owe their origin to the study of sound localization by humans, even though little is known about the physiological properties of the human auditory system. One of these ideas is binaural cross-correlation which assumes that the human brain performs a process similar to mathematical cross-correlation to measure the interaural time difference for localization in the horizontal plane. The most complete set of neural evidence for this theory comes from the study of sound localization and its brain mechanisms in barn owls, although partial support is also available from studies on laboratory mammals. Animal models of human sensory perception make two implicit assumptions; animals and humans experience the same percept and the same neural mechanism underlies the creation of the percept. These assumptions are hard to prove for obvious reason. This article reviews several lines of evidence that similar neural mechanisms must underlie the perception of sound locations in humans and owls. © 2000 Elsevier Science Inc. All rights reserved.

*Keywords:* Sound localization; Owls; Humans; Cross correlation

## 1. Localization of illusory sound sources

Both humans and owls use the interaural time difference (ITD) for localization in the horizontal plane. When the ITD is zero in signals delivered by earphones, the source appears at the midpoint between the ears. As the ITD is varied, the source appears to shift towards the ear at which the

signal arrives earlier. This simple relationship between ITD and location holds when signal bandwidth is broad. With narrowband signals both humans and owls may perceive sounds coming from directions other than those of real sources (Sayers and Cherry, 1957; Bernstein and Trahiotis, 1985; Stern and Trahiotis, 1997; Saberi et al., 1998a, 1999).

If the sound incidence angles encoded by ITDs are known, the cross-correlation theory can predict from ITDs and tonal period where phantom sources occur. Cross-correlation of a pair of tones

<sup>☆</sup> Plenary lecture at the International Congress of Comparative Physiology and Biochemistry in August 1999, Calgary, Alta, Canada.

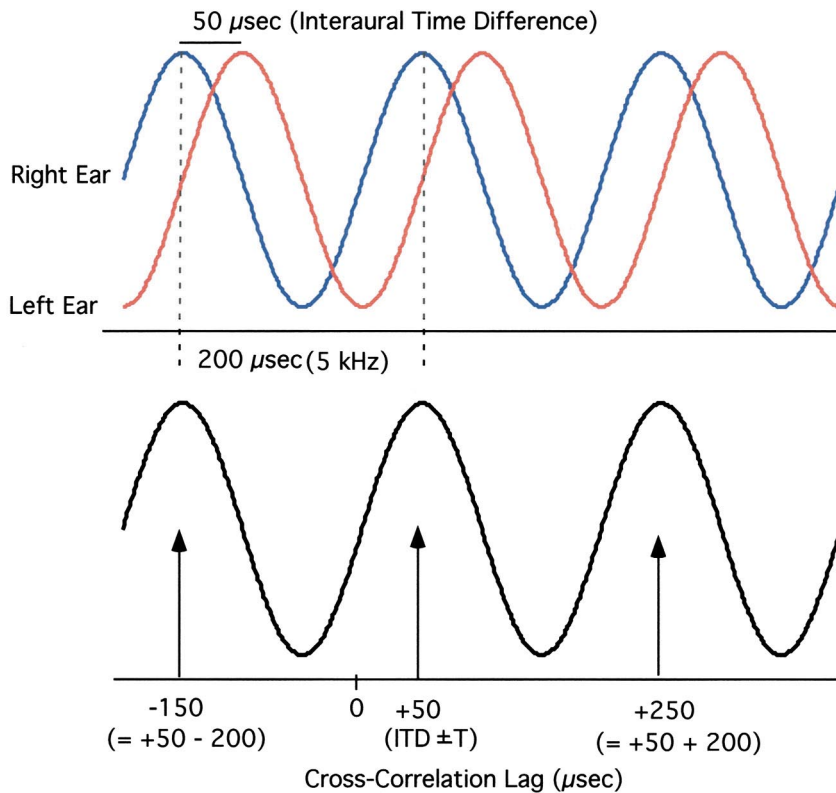


Fig. 1. Cross-correlation of narrowband signals. The right signal leads the left one by 50  $\mu\text{s}$  which is the interaural time difference (ITD). Note that the wave front reaches both ears simultaneously, i.e. no onset time difference. The two signals match with each other, when the right signal is delayed by 50  $\mu\text{s}$  or when the left signal is delayed by 150  $\mu\text{s}$  (from 50–200  $\mu\text{s}$ ). The peaks of correlogram occur at lag time corresponding to ITD and  $\text{ITD} \pm T$ , where  $T$  is the period of the stimulus tone.

containing an ITD shows multiple peaks which occur at time lags corresponding to the ITD and  $\text{ITD} \pm nT$ , where  $T$  is the period of the stimulus tone and  $n$  is an integer (Fig. 1). However,  $n$  is usually 1, because  $n = 2$  for all usable frequencies exceeds the owl's maximal ITD of 200  $\mu\text{s}$ . In the owl's auditory system, 50 and 150  $\mu\text{s}$  represent 20 and 50°, respectively (Moiseff and Konishi, 1981; Moiseff, 1989). A burst of 5-kHz tone emanating from a speaker at +20° (+ meaning right side of the midline) may cause owls to turn its heads towards -50° (- meaning left side of the midline) (Saber et al., 1999). The cross-correlation lags at which peaks occur are +50  $\mu\text{s}$  which is the ITD and  $50 \pm 200 \mu\text{s}$ . Note that  $50 - 200 \mu\text{s} = -150 \mu\text{s}$  which codes for -50°.

When waveforms are complex, cross-correlation of such signals shows only one peak at a lag corresponding to the ITD in the signal. Thus, neither humans nor owls perceive illusory sound sources, when signal bandwidth is broader than a

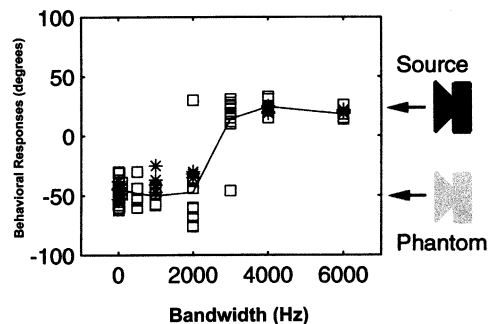


Fig. 2. Effects of signal bandwidth on sound localization by owls. Both humans and owls localize illusory sound sources in response to narrowband signals such as tones. In this study, the speaker was located at 20° to the right of the owl or an ITD of +50  $\mu\text{s}$  was delivered by earphones. Bandwidth was varied from 0 (i.e. tone) to 6 kHz with reference to a center frequency of 5 kHz. The owl turned its head towards a phantom source at 50° to the left when bandwidth was less than 3 kHz. As bandwidth increased beyond 3 kHz, the owl always localized the real source. Each square shows one trial in free field and each asterisk shows one trial with earphones (adapted from Saber et al., 1999).

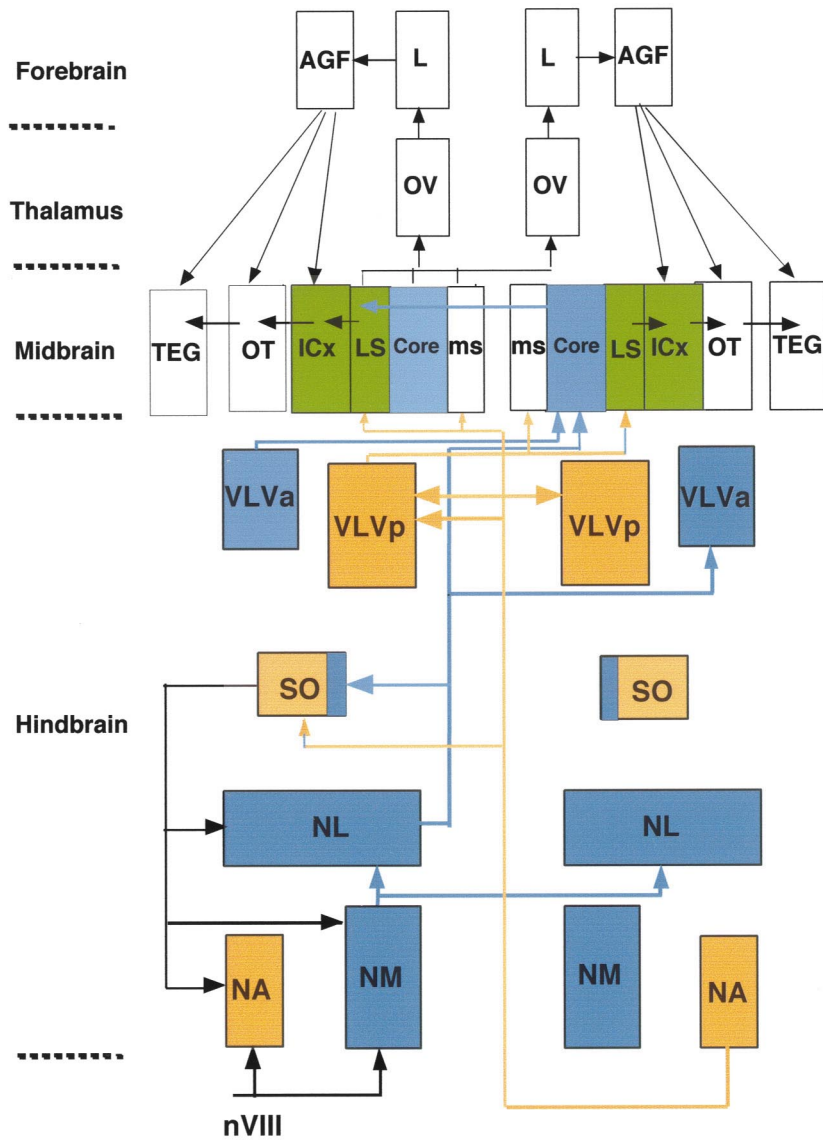


Fig. 3. Time and intensity processing pathways of the owl's auditory system. This shows only the brain areas whose role in sound localization is known and the connections that indicate ipsilateral or contralateral projections. The owl's auditory system processes ITD and IID in separate parallel pathways. Each primary auditory fiber (nVIII) divides into two branches, one innervates cochlear nucleus angularis (NA) and the other cochlear nucleus magnocellularis (NM). These two nuclei are the starting stations for the two pathways as indicated by blue and brown areas and connections. Nucleus laminaris (NL) which receives inputs from the left and right magnocellular nuclei is the first site for processing ITD. NL projects contralaterally to one of the lemniscal nuclei (VLVa) and the core of the central nucleus of the inferior colliculus. The core projects to the lateral shell (LS) on the contralateral side where the two pathways meet as shown by green. The time and intensity pathways and different frequency bands converge in the external nucleus of the inferior colliculus (ICX). This area contains a map of auditory space which is composed of neurons selective for combinations of ITD and IID. This map projects to the optic tectum (OT) to form a bimodal map of space. The optic lobe also contains a motor map which controls head turning behavior through the midbrain tegmentum (TEG). This tectal pathway can support sound localization in the absence of signals from the forebrain. However, the forebrain alone can also support sound localization behavior without the tectal pathway. The inferior colliculus projects to nucleus ovoidalis (OV) in the thalamus which in turn projects to Field L in the forebrain. Field L projects to the archistriatal area (AGF) which can control the turning of the head during sound localization (based on Knudsen, 1982; Takahashi and Konishi, 1988a,b; Carr et al., 1989; Olsen et al., 1989; Takahashi et al., 1989; Masino and Knudsen, 1990, 1993; Knudsen et al., 1993, 1995; Cohen and Knudsen, 1994, 1995).

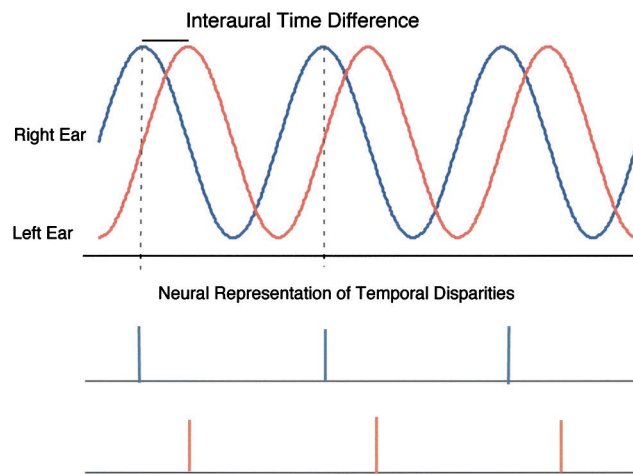


Fig. 4

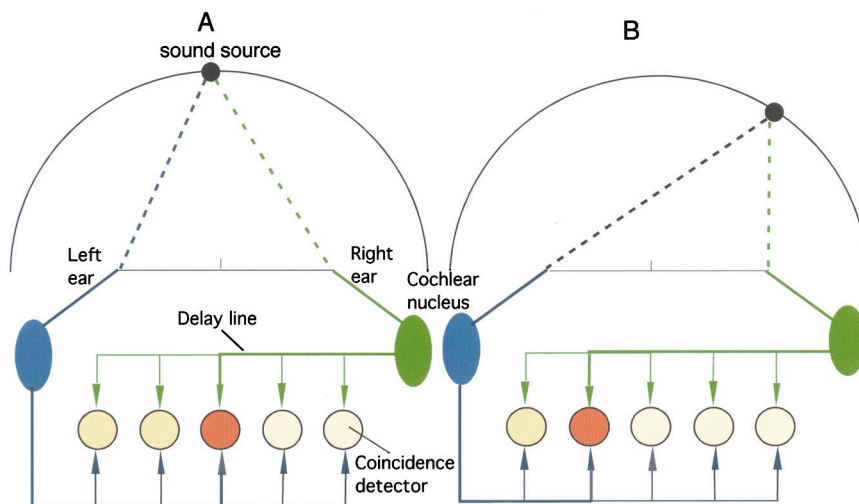


Fig. 5

Fig. 4. Neural coding of time. To encode time both birds and mammals use impulses that occur at particular phase angles of tones or spectral components of complex sounds.

Fig. 5. A neural model of cross-correlation. Cross-correlation requires means to delay one or both trains of impulses and devices to measure the degree of match between the left and right trains. This figure shows a model which satisfies the above requirements. The coincidence detectors are neurons that measure the degree of match between the two signals. The lines that reach these neurons represent the axonal delay lines, the length of which varies systematically from one end of the neuron array to the other. Panel A shows the center coincidence detector (dark brown) responding best to a signal coming from a point equidistant to the two ears, because acoustic delay + neural conduction delay for the two sides is the same. In panel B, because the sound source is nearer to the right ear than to the left ear, the site of maximal discharge shifts towards the left in the array.

certain value which is 300 Hz in humans and 3 kHz in owls (Fig. 2) (Stern et al., 1988; Saberi et al., 1999). This difference is correlated with the frequency range in which each species can use ITD for localization. Owls can use ITD for sound localization at frequencies as high as 8.5 kHz, whereas the highest frequency for humans is ~ 1200 Hz.

## 2. Neural correlates of illusory localization and its elimination

In owls, we can study the neural bases for both the illusion and the methods of eliminating it. The discussion of these issues requires a review of the owl's auditory system. The avian cochlea performs frequency decomposition of complex

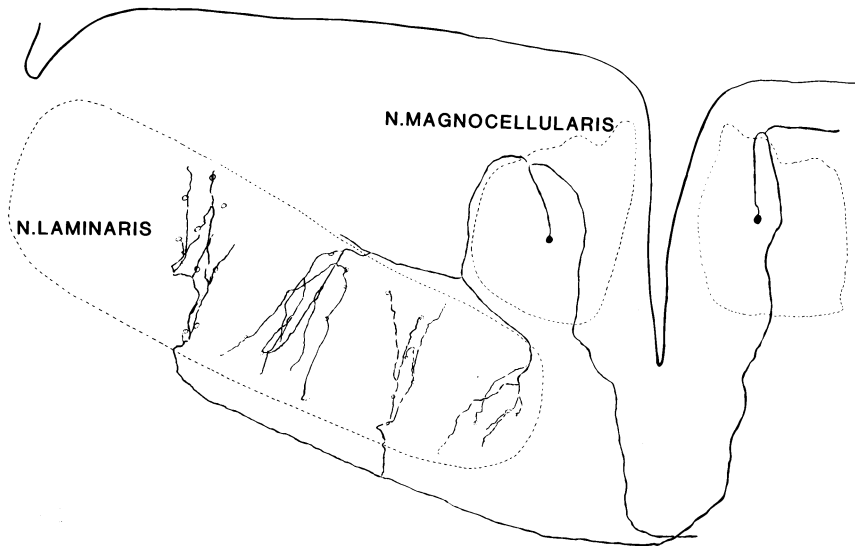


Fig. 6. Axonal delay lines and coincidence detection. In the owl's auditory system, axons from nucleus magnocellularis serve as delay lines and nucleus laminaris cells work as coincidence detectors. This figure shows a reconstruction of an axon and its branches from each side. The lines are axons and the circles are laminaris cell bodies. Nucleus laminaris is tonotopically organized and the detection of ITDs occurs separately in different frequency bands (from Konishi et al., 1988).

sounds, as does the mammalian ear. Of the three attributes of sounds, place along the basilar membrane encodes frequency, the rate of discharge encodes amplitude, and phase-locked impulses encode phase. The owl's auditory system processes ITDs and IIDs (interaural intensity differences) in separate parallel pathways extending from the cochlear nuclei, the first auditory stations in the brain, to the midbrain where the two pathways unite (Fig. 3) (review in Konishi, 1995). Owls use IIDs for localization in the vertical plane (Knudsen and Konishi, 1980; Moiseff, 1989).

Temporal disparities between left and right trains of phase-locked impulses provide the data for extracting ITDs (Fig. 4). Jeffress (1948) put forth a model for the detection of ITDs (Fig. 5). His method uses delay lines and an array of coincidence detectors to measure the degree of match between the two trains. This operation is similar to cross-correlation. Furthermore, he proposed that the place of coincidence detectors in the array encodes the direction of sound sources. This hypothesis involves a transformation of codes from time to place. In the barn owl's auditory system, the axons from nucleus magnocellularis serve as delay-lines and the somata of nucleus laminaris (NL) serve as coincidence detectors (Fig. 6). Similar circuits are found in the

medial superior olivary nucleus (MSO) of mammals (Smith et al., 1998).

Both NL and MSO neurons respond best when impulses from the two ears arrive in synchrony which occurs when the leading sound is delayed by ITD and ITD +  $T$  or when the lagging sound is delayed by ITD -  $T$  (Goldberg and Brown, 1969; Carr and Konishi, 1990; Yin and Chan,

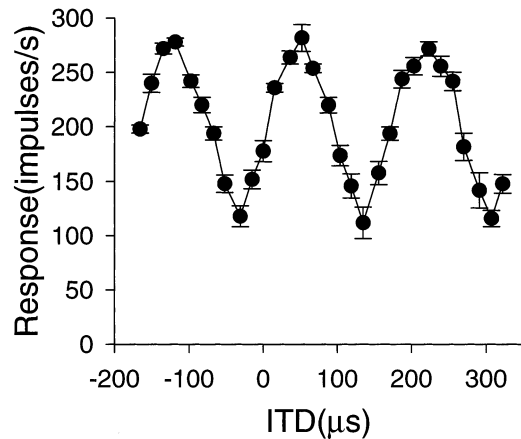


Fig. 7. ITD curve and phase-ambiguity. An ITD curve is a plot of the discharge rate of a single neuron as a function of ITD. This example is from nucleus laminaris. Note that this neuron responded to more than one ITD. This phenomenon is called phase-ambiguity. The distance between the peaks is the same as the period of the stimulus tone (adapted from Peña et al., 1996).

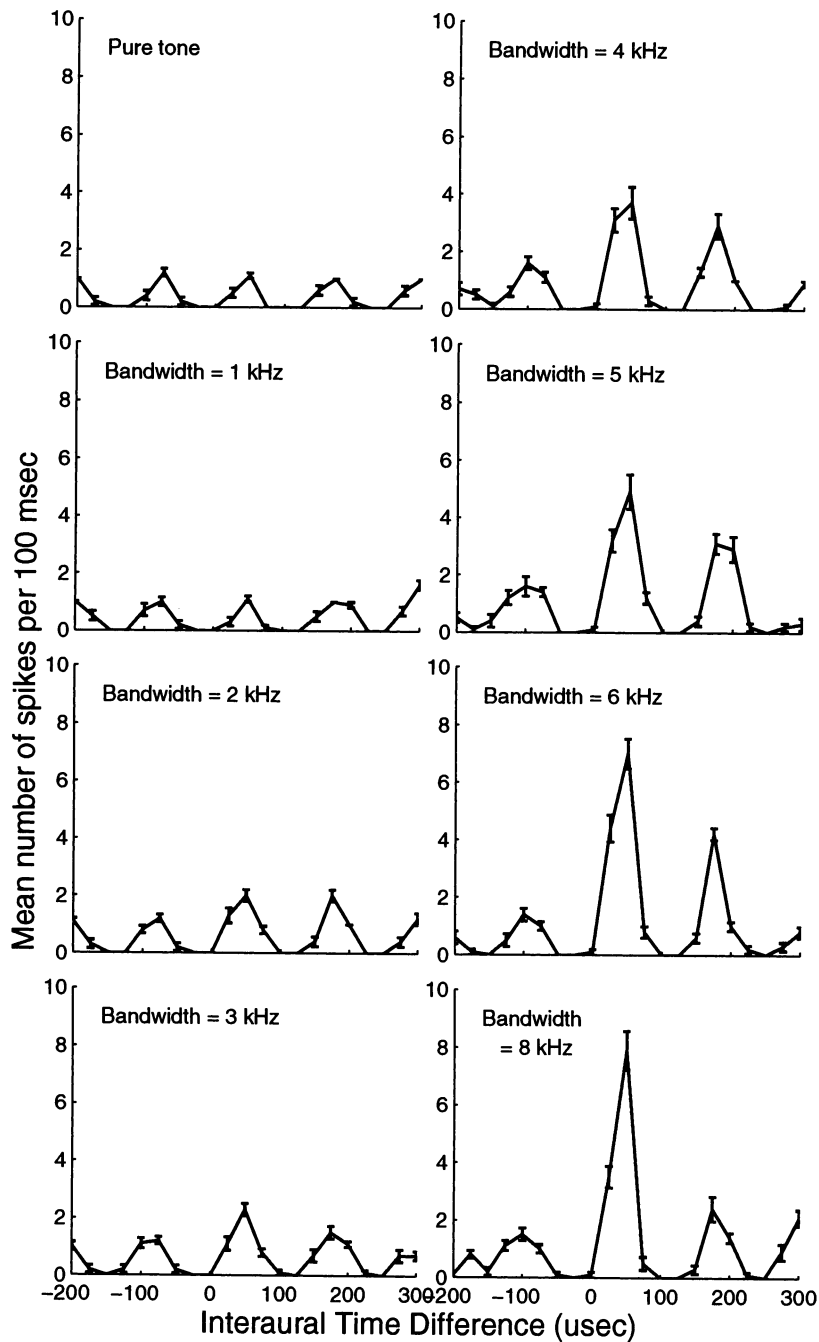


Fig. 8. Effects of bandwidth on ITD responses of a single neuron. This tectal neuron showed phase-ambiguity when the stimulus was narrowband. As signal bandwidth increased, the response peak corresponding to the stimulus ITD grew, while other peaks remained unchanged (adapted from Saberi et al., 1999).

1990). The responses of coincidence detectors are not all or nothing but graded according to the degree of departure from coincidence. Thus, a plot of discharge rate against ITD looks like a sine curve with peaks at ITD and  $ITD \pm T$  and

troughs at  $180^\circ$  away from the peaks (Fig. 7). Such a graph will be referred to as an ITD curve. All NL and MSO neurons show the same response pattern irrespective of stimulus bandwidth, because each neuron is tuned to a narrow range

of frequencies. The ear decomposes complex sounds into their frequency components on which NL and MSO perform cross-correlation. Now the question is how the auditory system distinguishes ITD from  $ITD \pm T$ .

Human psychoacousticians proposed a scheme that would solve this problem. ITD is independent of frequency, whereas  $ITD \pm T$  varies with frequency, because  $T$  changes with frequency. Therefore, comparison of ITD responses of neurons across different frequency bands should discriminate between frequency-dependent and -independent ITDs. How this comparison is carried out in the human brain has been a subject of debate (Shackleton et al., 1992; Trahiotis and Stern, 1994). In the owl, one can observe the

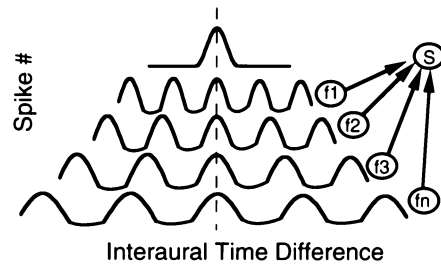


Fig. 10. Detection of frequency independent ITD by frequency convergence. An ICX neuron (S) receives inputs from lower-order neurons tuned to the same ITD, although they prefer different frequencies ( $f_1$ – $f_n$ ). ITD curves for different frequencies align only at the ITD common to all neurons. Note that the peaks representing  $ITD \pm T$  do not match across frequencies. Summing of these curves will give rise to a large peak at the frequency independent ITD, whereas the other peaks and troughs cancel each other out. Other mechanisms such as inhibition are also involved in reducing peaks other than the one at the frequency independent ITD (from Konishi, 1992).

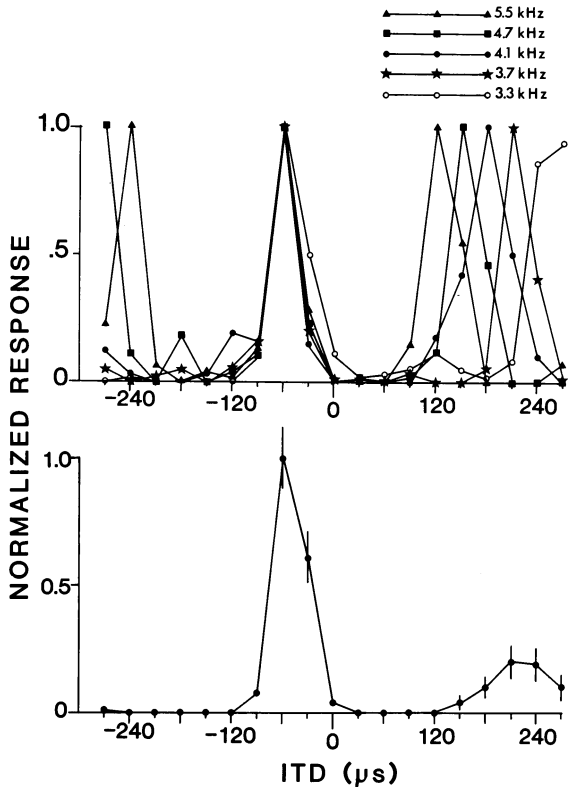


Fig. 9. Detection of frequency independent ITD. Both human and the owl's auditory system discriminates between ITD and  $ITD \pm T$  by comparing ITD responses across different frequencies. This process can be seen in this ICX neuron. The frequency independent ITD in this case is  $-60 \mu\text{s}$  to which the neuron responded regardless of stimulus frequency, whereas other response peaks varied with frequency (top panel). The same neuron responded only to  $-60 \mu\text{s}$  when the ITD was conveyed by a broadband signal (bottom panel) (from Konishi et al., 1988).

process at the level of single neurons in the inferior colliculus. In one part of the inferior colliculus known as the external nucleus (ICX), different frequency bands carrying ITD information converge on single neurons (cf. Fig. 3). The effects of the convergence can be observed there and in the optic tectum that receives input from ICX (Knudsen, 1982). For example, the ITD curve of an optic tectum neuron shows multiple peaks, when the signal is narrowband. As signal bandwidth increases, the peak for the stimulus ITD grows taller than the peaks for  $ITD \pm T$  (Fig. 8). The difference between the main and side peaks varies with signal bandwidth. The wider the band, the larger the difference (Mazer, 1998). The difference between the main and side peaks becomes statistically significant when signal bandwidth exceeds 3 kHz (Saber et al., 1999). Recall that this is also the bandwidth above which the owls always localized the true source.

We can explain how the convergence of different frequency bands results in the differential growth of the main peak. When ICX neurons receive signals from lower-order neurons tuned to different frequencies, they gather input from those tuned to the same ITD. However, because the afferent neurons respond to  $ITD \pm T$ , they confer this property upon the ICX neurons. Fig. 9 shows the response of an ICX neuron to noise (lower panel) and tones (upper panel). The neuron re-

sponds to the stimulus ITD of  $-60 \mu\text{s}$  regardless of the stimulus frequency. The side peaks occur at  $\text{ITD} \pm T$  in which  $T$  varies with frequency. The ITD curve of the same neuron obtained with a broadband stimulus shows one large peak at the same stimulus ITD and a small peak elsewhere. This observation allows us to create a model of frequency convergence as shown in Fig. 10. An ICX neuron (S) receives inputs from lower-order neurons tuned to different frequency bands ( $f_1$ – $f_n$ ). All these neurons respond to the same ITD as shown by the dashed line. When the ICX neuron adds the inputs across all frequency bands, the peaks at the frequency-independent ITD add, whereas the peaks and troughs of  $f_1$ – $f_n$  cancel each other out. This linear summation across frequency is not the only method that the owl's auditory system uses. Evidence indicates that non-linear integration such as inhibition is also involved (Takahashi and Konishi, 1986; Fujita and Konishi, 1991; Mori, 1997).

### 3. The effects of de-correlation on sound localization

Humans and owls fail to localize signals that are uncorrelated between the ears, because cross-correlograms of such signals do not contain peaks at any time lag. Addition of random noise to correlated signals reduces the degree of correlation. The amplitude difference between the correlated and random noise determines the degree of correlation (Jeffress and Robinson, 1962). In humans, partially correlated signals produce a blurred image inside the brain and the blur increases, as the signals are further decorrelated (Blauert and Lindemann, 1986). Jeffress et al. (1962) carried out experiments in which human subjects used an electronic delay device to bring a sound image to the midpoint between the ears from an arbitrary initial locus. As the degree of correlation became smaller than  $\sim 0.2$ – $0.3$ , the subjects' choice of delays became more variable, i.e. the standard deviations of the mean delays chosen by the subjects increased. Using partially

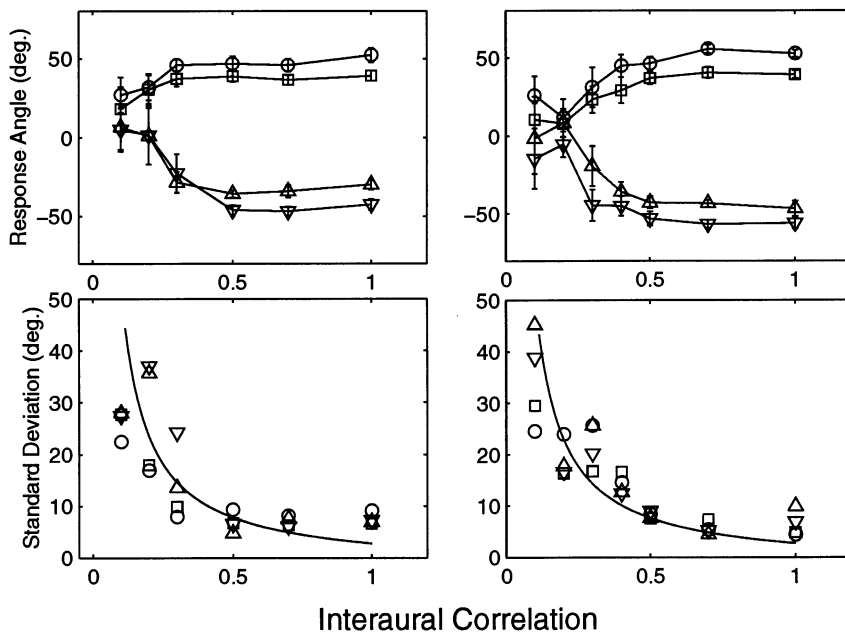


Fig. 11. Effects of signal decorrelation on sound localization. The top panels show the mean head angles of two owls as a function of ITD and interaural correlation. Four values of ITD were used and are indicated by symbols; inverted triangle,  $-150 \mu\text{s}$ ; triangles,  $-100 \mu\text{s}$ ; squares,  $+100 \mu\text{s}$ ; circles,  $+150 \mu\text{s}$ . Error bars indicate one standard deviation. The bottom panels plot the standard deviation of the means against interaural correlation. The solid curves in these panels indicate  $\delta\rho^{-1}$  as explained in the text (adapted from Saberi et al., 1998b).

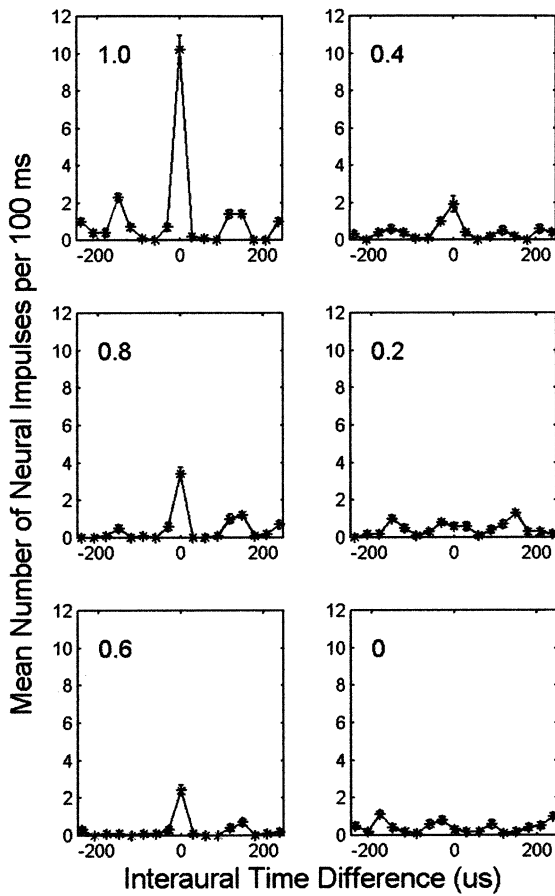


Fig. 12. Effects of signal decorrelation on ITD responses of a single neuron. Different panels show how the main peak in the ITD curve became smaller as interaural correlation was decreased (adapted from Saberi et al., 1998b).

correlated signals, we studied how owls localize such signals. We obtained both the mean localization angles and the standard deviations of the means (Fig. 11). The standard deviations remained almost constant until the degree of correlation decreased to  $\sim 0.2$ – $0.3$ . The curves for the standard deviations closely resemble that obtained for humans (Jeffress et al., 1962). Thus, humans and owls performed similarly in similar perceptual tasks.

#### 4. The effects of decorrelation at the level of single neurons

In owls, the effects of decorrelation can be studied at the level of single neurons (Albeck and Konishi, 1995; Saberi et al., 1998b). Neurons of

the external nucleus and optic tectum respond to correlated broadband signals with ITD curves containing a tall main peak and small or no side peaks. As the signal is gradually decorrelated, the main peak becomes smaller until it is no longer recognizable (Fig. 12). This occurs when the degree of correlation is between 0.2 and 0.4. Using a sample of neurons such as shown in Fig. 13, we studied the extent to which the statistical properties of neuronal responses can account for the distribution of standard deviations in the behavioral data. The owl's ability to detect an ITD depends on the number of neurons tuned to that ITD, their discharge rates, and the variability of these rates. Thus, the following equation  $\delta_{\rho}^{-1} = \frac{\sum Y_{i\rho} - \sum Y_{i0}}{\sqrt{\sum \text{VAR}(Y_{i\rho}) + \sum \text{VAR}(Y_{i0})}}$  is one way to represent the detectability of an ITD for different interaural correlations (where  $Y_{i\rho}$  is mean discharge rate for neuron  $i$  and interaural correlation of  $\rho$ ,  $Y_{i0}$  is mean discharge rate for neuron  $i$  and interaural correlation of zero, VARs indicate the variances associated with the respective means). Because ITD is not detectable when interaural correlation is zero,  $Y_{i0}$  indicates mean spontaneous discharge rates.  $\delta_{\rho}^{-1}$  has a distribution that resembles that of the standard deviation of behavioral results (cf. Fig. 11). Note that  $\delta_{\rho}^{-1}$  and the behavioral standard deviation vary similarly for low values of  $\rho$ . On the other hand,  $\delta_{\rho}^{-1}$  approaches zero as  $\rho$  nears 1, whereas the behavioral standard deviation never reaches zero. This relationship suggests that factors beyond the optic tectum are limiting the consistency of behavioral performance. In addition to neural noise, errors in decision-making and head turning may also account for the discrepancy.

#### 5. Concluding remarks

The examples presented in this article show that combinations of theory, behavioral and neurophysiological studies in animals can make meaningful contributions to the understanding of sensory perception by humans. We could establish these examples, because humans and owls use the same method of detecting ITD, i.e. binaural cross-correlation. This theory can predict the effects of decorrelation and bandwidth on both behavioral performance and neuronal responses. Furthermore, anatomical and physiological knowledge about the owl's auditory system greatly facilitated

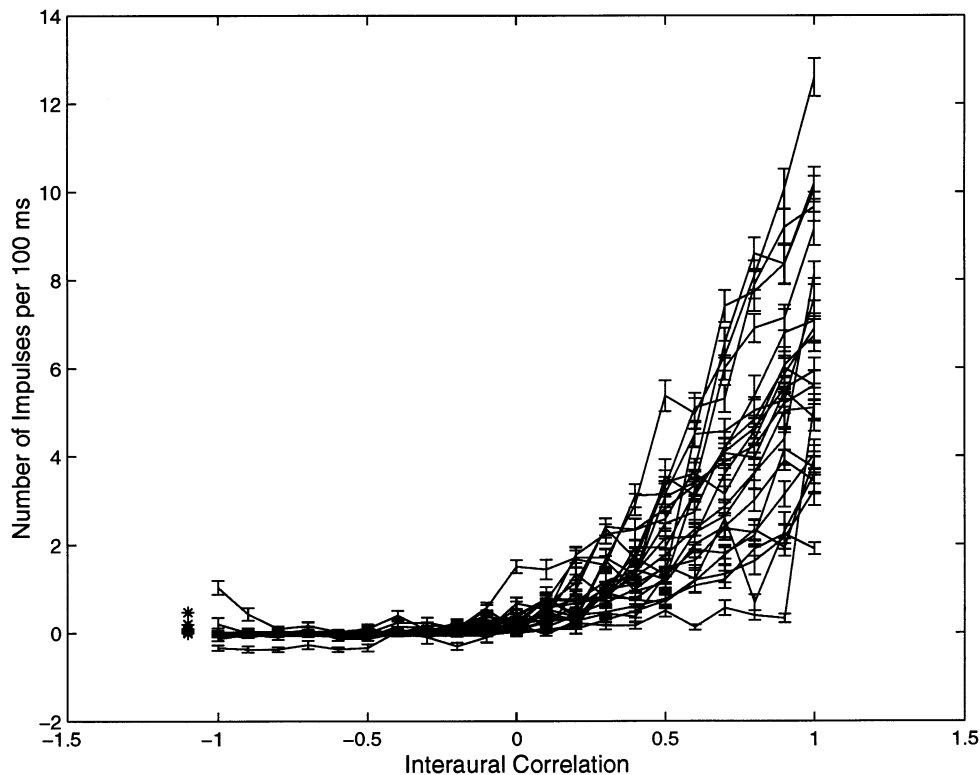


Fig. 13. Effects of decorrelation on ITD responses of a sample of tectal neurons. This graph plots the height of the main ITD peak as a function of interaural correlation. Each line connects mean discharge rates of a neuron. Vertical bars show the standard deviations of the means. All neurons ceased to respond to the stimulus when interaural correlation was zero or smaller than zero. As interaural correlation increased, their discharge rates rose rapidly (adapted from Saberi et al., 1998b).

the collection of relevant neural data. As is well established in vision research, perceptual illusions that humans and animals share are powerful tools for the kinds of comparative approaches used in the present paper.

#### Acknowledgements

I thank Chris Malek for his assistance. This work was supported by a grant from the National Institutes of Deafness and Other Communicative Disorders.

#### References

- Albeck, Y., Konishi, M., 1995. Responses of neurons in the auditory pathway of the barn owl to partially correlated binaural signals. *J. Neurophysiol.* 74, 1689–1700.
- Bernstein, L.R., Trahiotis, C., 1985. Lateralization of sinusoidally amplitude-modulated tones: effects of spectral locus and temporal variation. *J. Acoust. Soc. Am.* 78, 514–523.
- Blauert, J., Lindemann, W., 1986. Spatial mapping of intercranial auditory events for various degrees of interaural coherence. *J. Acoust. Soc. Am.* 79, 806–813.
- Carr, C.E., Konishi, M., 1990. A circuit for detection of interaural time differences in the brain stem of the barn owl. *J. Neurosci.* 10, 3227–3246.
- Carr, C.E., Fujita, I., Konishi, M., 1989. Distribution of GABAergic neurons and terminals in the auditory system of the barn owl. *J. Comp. Neurol.* 286, 190–207.
- Cohen, Y.E., Knudsen, E.I., 1994. Auditory tuning for spatial cues in the barn owl basal ganglia. *J. Neurophysiol.* 72, 285–298.
- Cohen, Y.E., Knudsen, E.I., 1995. Binaural tuning of auditory units in the forebrain archistriatal gaze fields of the barn owl: local organization but no space map. *J. Neurosci.* 15, 5152–5168.
- Fujita, I., Konishi, M., 1991. The role of GABAergic inhibition in processing of interaural time difference in the owl's auditory system. *J. Neurosci.* 11, 722–739.
- Goldberg, J.M., Brown, P.B., 1969. Response of binau-

- ral neurons of dog superior olivary complex to dichotic stimuli: some physiological mechanisms of sound localization. *J. Neurophysiol.* 32, 613–636.
- Jeffress, L.A., Robinson, D.A., 1962. Formulas for the coefficient of interaural correlation for noise. *J. Acoust. Soc. Am.* 34, 1658–1659.
- Jeffress, L.A., Blodgett, H.C., Deatherage, B.H., 1962. Effect of interaural correlation on the precision of centering a noise. *J. Acoust. Soc. Am.* 32, 1122–1123.
- Knudsen, E.I., 1982. Auditory and visual maps of space in the optic tectum of the owl. *J. Neurosci.* 2, 1177–1194.
- Knudsen, E.I., Knudsen, P.F., Masino, T., 1993. Parallel pathways mediating both sound localization and gaze control in the forebrain and midbrain of the barn owl. *J. Neurosci.* 13, 2837–2852.
- Knudsen, E.I., Konishi, M., 1980. Monaural occlusion shifts receptive-field locations of auditory midbrain units in the owl. *J. Neurophysiol.* 44, 687–695.
- Knudsen, E.I., Cohen, Y.E., Masino, T., 1995. Characterization of a forebrain gaze field in the archistriatum of the barn owl: microstimulation and anatomical connections. *J. Neurosci.* 15, 5139–5151.
- Konishi, M., 1992. The neural algorithm for sound localization in the owl. *Harvey Lectures Ser.* 86, 47–64.
- Konishi, M., 1995. Neural mechanisms of auditory image formation. In: Gazzaniga, M.S. (Ed.), *The Cognitive Neurosciences*. MIT Press, Cambridge, MA, pp. 269–277.
- Konishi, M., Takahashi, T., Wagner, H., Sullivan, W.E., Carr, C.E., 1988. Neurophysiological and anatomical substrates of sound localization in the owl. In: Edelman, G., Gall, W.E., Cowan, W.M. (Eds.), *Auditory Function: Neurobiological Bases of Hearing*. Wiley, New York, pp. 721–745.
- Masino, T., Knudsen, E.I., 1990. Horizontal and vertical components of head movement are controlled by distinct neural circuits in the barn owl. *Nature* 345, 434–437.
- Masino, T., Knudsen, E.I., 1993. Orienting head movements resulting from electrical microstimulation of the brainstem tegmentum in the barn owl. *J. Neurosci.* 13, 351–370.
- Mazer, J.A., 1998. How the owl resolves auditory coding ambiguity. *Proc. Natl. Acad. Sci. USA* 95, 10932–10937.
- Moiseff, A., 1989. Bi-coordinate sound localization by the barn owl. *J. Comp. Physiol. A* 164, 637–644.
- Moiseff, A., Konishi, M., 1981. Neuronal and behavioral sensitivity to binaural time differences in the owl. *J. Neurosci.* 1, 40–48.
- Mori, K., 1997. Across-frequency non-linear inhibition by GABA in processing of interaural time difference. *Hear. Res.* 111, 22–30.
- Olsen, J.F., Knudsen, E.I., Esterly, S.D., 1989. Neural maps of interaural time and intensity differences in the optic tectum of the barn owl. *J. Neurosci.* 9, 2591–2605.
- Saberi, K., Farahbod, H., Konishi, M., 1998a. How do owls localize interaurally phase-ambiguous signals? *Proc. Natl. Acad. Sci. USA* 95, 6465–6468.
- Saberi, K., Takahashi, Y., Konishi, M., Albeck, Y., Arthur, B.J., Farahbod, H., 1998b. Effects of interaural decorrelation on neural and behavioral detection of spatial cues. *Neuron* 21, 789–798.
- Saberi, K., Takahashi, Y., Farahbod, H., Konishi, M., 1999. Neural bases of an auditory illusion and its elimination in owls. *Nat. Neurosci.* 2, 656–659.
- Sayers, B.M., Cherry, E.C., 1957. Mechanism of binaural fusion in the hearing of speech. *J. Acoust. Soc. Am.* 29, 973–987.
- Shackleton, T.M., Meddis, R., Hewitt, M.J., 1992. Across-frequency integration in a model of lateralization. *J. Acoust. Soc. Am.* 91, 2276–2279.
- Smith, P.H., Joris, P.X., Yin, T.C., 1998. Anatomy and physiology of principal cells of the medial nucleus of the trapezoid body (MNTB) of the cat. *J. Neurophysiol.* 79, 3127–3142.
- Stern, R.M., Trahiotis, T., 1997. Models of binaural perception. In: Gilkey, R.H., Anderson, T.R. (Eds.), *Binaural and Spatial Hearing*. Erlbaum, Mahwah, NJ, pp. 499–531.
- Stern, R.M., Zeiberg, A.S., Trahiotis, C., 1988. Lateralization of complex binaural stimuli: a weighted-image model. *J. Acoust. Soc. Am.* 84, 156–165.
- Takahashi, T., Konishi, M., 1986. Selectivity for interaural time difference in the owl's midbrain. *J. Neurosci.* 6, 3413–3422.
- Takahashi, T.T., Konishi, M., 1988a. Projections of nucleus angularis and nucleus laminaris to the lateral lemniscal nuclear complex of the barn owl. *J. Comp. Neurol.* 274, 212–238.
- Takahashi, T.T., Konishi, M., 1988b. Projections of the cochlear nuclei and nucleus laminaris to the inferior colliculus of the barn owl. *J. Comp. Neurol.* 274, 190–211.
- Takahashi, T., Wagner, H., Konishi, M., 1989. Role of commissural projections in the representation of bilateral auditory space in the barn owl's inferior colliculus. *J. Comp. Neurol.* 281, 545–554.
- Trahiotis, C., Stern, R.M., 1994. Across-frequency interaction in lateralization of complex binaural stimuli. *J. Acoust. Soc. Am.* 96, 3804–3806.
- Yin, T.C.T., Chan, C.K., 1990. Interaural time sensitivity in medial superior olive of cat. *J. Neurophysiol.* 64, 465–487.